A Patch Ordering Approach to Single Image Super-Resolution Problem

Vahid Anari[1], Farbod Razzazi[1*], Rasoul Amirfattahi[2]
1- Department of Electrical and Computer Engineering, Science and Research Branch, Islamic Azad University, Tehran, Iran.
Email: vanari1361@gmail.com, razzazi@srbiau.ac.ir (Corresponding author)
2- Department of Electrical and Computer Engineering, Isfahan University of Technology, Isfahan, Iran, 84156-83111.
Email: fattahi@cc.iut.ac.ir

Received: May 2019 Revised: July 2019 Accepted: September 2019

ABSTRACT:
In this paper, we propose a novel patch ordering approach to Single Image Super-Resolution (SR) algorithm which is called as Patch Ordering Approach to Single Image Super Resolution (POSR). We aimed at selecting more informative High-Resolution (HR) and Low-Resolution (LR) patches for single image SR algorithms based on sparse representation and dictionary learning. Our proposed POSR algorithm, first ordered HR and LR patches for each training images based on minimization of total variation measure (TV). Then, it assigned a sampling step for patch selection in each image. In this way, training patches were extracted based on image texture complexity. This leads to training dictionaries with the high and low resolution more efficiently. Unlike other methods which have used additional restrictions in high resolution image reconstruction phase, proposed method, has only used the basic assumption of sparse representation super resolution. The experimental results for quantitative criteria (PSNR, RMSE, SSIM and elapsed time), human observation as a qualitative measure and computational complexity verify the improvements offered by the proposed POSR algorithm.

KEYWORDS: Dictionary Learning, Sparse Representation, Super Resolution, Patch Ordering.

1. INTRODUCTION

In recent years, SR has been regarded as one of the most interested research areas in digital image processing. Aside from that, resolution enhancement has been implemented by increasing the capability of imaging systems. SR is a software-based technology that reconstructs a HR image using single or multiple LR images. Among these methods, Single Image Super Resolution (SISR) refers to techniques that use single input LR image. Nowadays, SISR is widely used in many applications such as medical imaging systems, remote sensing, surveillance cameras, web technology, and cell phones. SR techniques can be classified into three categories: interpolation- based techniques [1, 2], reconstruction-based techniques [3-7] and learning-based techniques [8-13]. Interpolation-based techniques have simple structure and low computational cost. However, the smoothness of output images and artifact production are considered as their significant weaknesses. Bilinear and bi-cubic interpolations are the most famous approaches in this category. Reconstruction- based techniques deal with the SR as an optimization problem. Their cost function has a general term for adapting HR and LR images and a regularization term in order to be ensured of finding the best answer to the problem. Suresh et al. have used an adaptive edge detector as a regularization term in order to preserve edges and sharp image texture information [7]. In a similar study, Chen et al. have used a Tikhonov regularization term for HR image reconstruction [3]. They also have used singular value decomposition in order to reduce the computation. Although their approach worked well in 2x magnification, however, their performance was decreased in larger magnification factors. Learning- based techniques are the third category of SISR algorithms. These methods use a learning dataset that includes paired LR-HR patches. This technique finds the closest LR patches of the input image to LR patches of the dataset. Then, the corresponding HR patches are extracted. In the next step, the output HR image is reconstructed by merging the resulted HR patches. The superiority of the learning-based method to other methods is the ability to reconstruct the HR image with a wider range of magnification factors regarding previous two approaches [10, 12, 13]. In addition, the output image quality in some image classes is better than previously mentioned methods [10-12]. The learning procedure of these approaches is considered as a crucial part of these methods and may be considered as the core of the

algorithm. This study presents a new learning -based SISR method by selecting appropriate samples for dictionary learning.

1.2. Review of Literature

In recent years, many SISR techniques have been developed based on sparse coding and dictionary learning method [10-13]. The first dictionary learning based on SISR has been proposed by Yang et al. [11]. Their method, which was called as Sparse Coding Based Super Resolution (SCSR), was dependent on the assumption that the corresponding HR-LR patches have a same sparse activation vector over HR and LR dictionaries. It included two phases; in the first phase, HR and LR dictionaries pair were learnt. In the second phase, HR image was reconstructed. They generalized the K-SVD dictionary learning method [14] for HR-LR pair dictionary learning, which was called as coupled dictionary learning. Recently, their work has been extended effectively in [13, 15-19]. Learning HR-LR patch pair selection is the first step of dictionary learning phase. Clearly, learning patch pair selection has a great effect on the performance of the SR algorithms and plays an important role in the methods which were mentioned above. At this point, given a huge number of all existing overlapping patches, patch selection is unavoidable. In order to avoid using too many patches that are less informative, Yang et al. divided the patches into general, saliency and edge areas. In this method, the number of extracted patches from each image is equal to the calculated ratio of the number of training patches. Zeyde et al. have used the standard deviation for patch pruning [13], Chen et al. have proposed a super resolution based on structure feature of image patches [3]. Yeganli has defined the Sharpness Measure (SM) of the image patch through the magnitude of the gradient operator to cluster while obtaining category dictionaries [20]. Meanwhile, the distortion of perceptions for texture region is higher than that of flat areas. Guan has used morphological component analysis (MCA) in order to decompose the image into structural components and texture components [21]. Jiang has used structure tensor as a powerful image analysis tool in order to describe the texture for image [22]. They have extracted information such as the edge and corner information using eigenvectors, and have used them in SR method. Liu et al. have proposed a multi-scale patch-based sparse representation method for the enhancing the texture component [23]. Zhang et al. proposed the adaptive mixed samples ridge regression (AMSRR) to effectively optimize learned dictionaries [24]. Lu et al. utilized Sparse Domain Selection method (SDS) and achieved accurate and stable HR image recovery [25]. Naderahmadian et al. modified the dictionary update step in online dictionary learning [26]. Other algorithms that have been proposed included classified dictionaries [27], sub-dictionary learning [28] and solo dictionary learning [29].

1.3. Motivation and Contribution

Although, sparsity based on SR algorithm have worked well until now, unfortunately the existing methods have not emphasized on the number of extracted patches from learning images. In addition, previous methods have used common criteria such as standard deviation for patch selection. Therefore, it seems necessary to propose a new method which processes the patches more effectively for dictionary learning in SR. This paper presents a novel patch selection method for dictionary learning and HR image reconstruction which is called as Patch Ordering Super Resolution (POSR). The idea of patch ordering was presented first in [30]. Using the patch ordering total variation measure (TV), we propose a patch selection method based on the image texture complexity. Assuming that each patch is a point for Traveling Salesman Problem (TSP), we suggest a greedy solution in order to find the optimum path between the patches as cities. After computing the TV measure for ordered patches from each image, it will be used as an efficient criterion for texture complexity and selection of the number of informative patches of each learning image. In this way, learning images that contain more information will have more contribution in the learning phase. Similar to general dictionary learning- based SR, POSR method needs to train a pair of dictionaries, after sampling learning patches based on the proposed ordering method. The K-SVD training algorithm [14] is applied to these patches, resulting in the LR dictionary. In HR image reconstruction phase, POSR algorithm solves the optimization problem for sparse representation of LR patches regarding LR trained dictionary using OMP algorithm [31]. The number of non-zero elements of sparse vector is restricted to a pre-defined value. Finally, HR image patches were obtained from the LR patches representation vector and HR dictionary. The main merits of our proposed POSR method can be summarized as follows:

- A novel technique for SR based on sparse representation and image patch extraction is proposed.
- An effective method is proposed for patch ordering procedure by adopting TSP over image patches. The patch selection procedure helps the learnt dictionary to be more efficient.
- The proposed POSR results could perform better in comparison with state-of-the-art and classic interpolation- based methods (bi-ubic SR, SCSR [12], SISU [13], ANR [33], AMSRR [24] and SDS [25]).

1.4. Paper Structure

The reminder of the paper is organized as follows. The proposed SR method based on patch ordering and dictionary learning is described in detail in section 2. Section 3 provides experiments on the performance of our proposed POSR with bi-cubic SR, SCSR [10], SISU [13], GR [33], ANR [33], AMSRR [24], and SDS [25] methods. The paper is concluded in section 4.

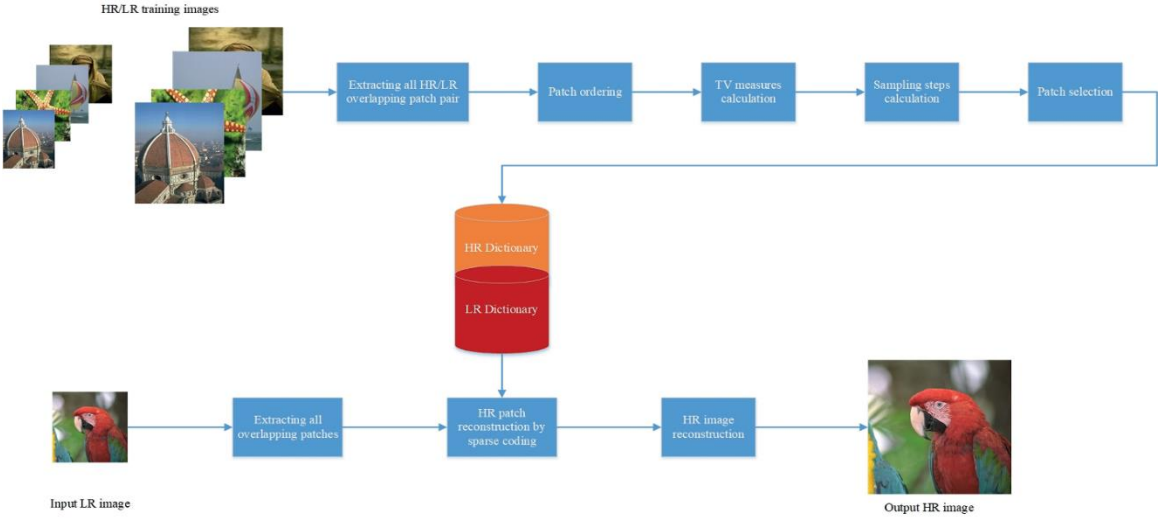

Fig. 1. steps involved in patch selection algorithm.

2. THE PROPOSED PATCH ORDERING BASED SUPER RESOLUTION (POSR)

This work aims at identifying informative patches from learning image dataset for SR purposes. Inspired from the study that has been proposed by Ram et al. [30], first we establish a patch selection approach based on ordering of patches, and then we deduce an SR algorithm based on selected patches.

2.1. Design of the Proposed Algorithm

In this section, due to the importance of patch selection in dictionary leaning and image super resolution through sparse recovery method, we pay more attention to patch selection stage of dictionary learning methods. In the first stage of our proposed algorithm, all of the extracted patches from an image are ordered by solving TSP. Then, by calculating total variance in measures for ordered patches, we assign the number of training patches for each image. Fig. 1 summarizes the steps which are involved in patch selection algorithm. For color images, considering that the human visual system is more sensitive to illuminance changes, patch ordering was applied to the illuminance channel only. After extracting informative patches for learning image dataset based on patch ordering, the next stage is LR dictionary training. Then, HR patch is restored using the same representative sparse vector. For this purpose, K-SVD method which was proposed by Aharon et al. [14] is employed using selected LR patches. After that, HR dictionary is obtained using the method which was proposed by Zeyde et al. in [13]. The final section of algorithm includes HR image reconstruction, these methods are described in detail in next sections.

2.2. Patch Selection based on Ordering

Let Y be an image of size $N_1 \times N_2$ and $\{y_k\}$ indicates the k^{th}overlapping patches with the size of $\sqrt{n} \times \sqrt{n}$. In the first stage, we extract all possible patches from the image. Assuming each patch is a point in the space; our goal is to re-order the patches in order to minimize the total variance (TV) measure:

$$\|\mathbf{y}\|_{TV} = \sum_{j=2}^{N_1 \times N_2} \left| y(j) - y(j-1) \right|. \quad (1)$$

The "smoothness" of ordered signal y^o can be measured using its TV.

Minimizing $\|y^o\|_{TV}$ comes down to find the shortest path that passes through the set of patches $\{y_k\}$, visiting each point only once. This can be regarded as an instance of the TSP [31], we choose a simple approximate solution, that is starting from a random point and then continuing from each patch y_i to its nearest neighbor $y_j$using Euclidean distance similarity measure.TV minimization of patches based on proposed patch ordering is summarized in the algorithm 1.

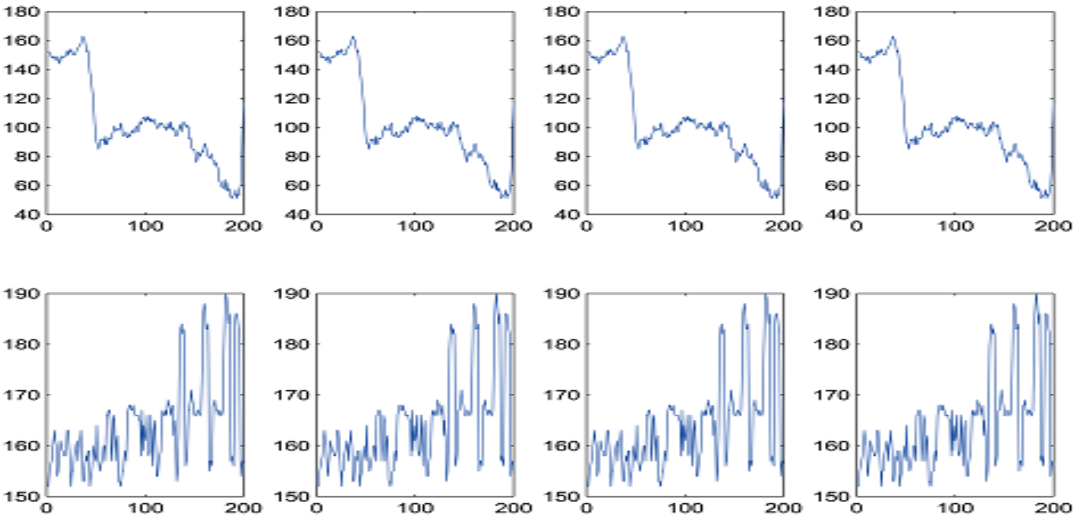

Fig. 1. Top row **(**left to right): The first to fourth pixels of the 10^5 ordered patches, bottom row (left to right): The first to fourth pixels of the original patches (vertical axis dedicated to pixel's illuminance value where horizontal axis are dedicated to pixel location).

Algorithm 1: proposed patch ordering based on greedy solution of TSP

Task: Reorder the image patches y_k

Parameters: We are given the $\sqrt{n}\times\sqrt{n}$ image patches: $\{y_k\}$, and the distance function ω.

Let A to be the set of indices of all overlapping patches, extracted from the image.

Initialization:

Choose the random index $i \in A$.

Set: r=1, $\Omega(r)=\{i\}$ $\Lambda(1)=\{i\}$

Main iteration:

For $j \in A$

Find y_j as the nearest neighbor to y_i

If $j \in A$ & $j \notin \Lambda$

Set $\Omega(r+1)=\{j\}$.

Else

Find y_j as the nearest neighbor to y_i such that $j \in A$ & $j \notin \Lambda$.

Set $\Omega(r+1)=\{j\}$.

Output: the set Ω holds the proposed patch ordering

The proposed patch ordering with the parameters n=4 and Euclidian similarity measure was applied to the patches of the Lena image with size of 256×256. We apply the obtained permutation to the column stacked version $\mathbf{y}$ of the Lena image, and obtain the reordered signal y^o. Then, we calculate the total variations of y and y^o. Results have shown that $\|y\|_{TV} = 7.56 \times 10^5$ and $\|y^o\|_{TV} = 1.74 \times 10^5$. It is obvious that TV measure was decreased to 77 percent. In order to demonstrate the regularity of the reordered signal visually, Fig. 2 shows the regularity of the reordered signal y^o compared to y.

After calculation of the TV measure for each image of data base, we assign the number of patch for each image which is proportional to its TV to total TV of images.

$$n_i = \frac{TV_i}{\sum_{j=1}^{M} TV_j} \times N, \qquad (2)$$

Where, n_i is number of the extracted patch from i^{th} image and $N$is the total numbers of training patches. After this step, we choose n_i patches simply and uniformly from each ordered image patches. Fig. 3 shows examples of training images and the results for the calculated TV measure, sampling step and number of extracting patches for each image are shown in table 1.

Fig. 3. Examples training images used for patch selection (a) Penguin, (b) boats, (c) old woman, (d) Ladybird and (e) Girls.

Table 1. TV measure, sampling step and number of extracted patches for sample images of Fig.3 (total number of training patches is 50000)

Image	Total variation	Sampling step	Number of extracted patches
Penguin		13	5044
Boats		10	6696
Old	1672	7	8974
Ladybird		12	5621
Girls		3	23662

2.3. Super Resolution based on Proposed Patch Selection

3.1.1.Dictionary learning using patch ordering

Patch selection of learning images is the first step for dictionary learning. Based on the method which was described in section 2-2, we have modified the dictionary learning method which was proposed in [13]. In our proposed method, the dictionaries are trained using selected patches and proposed patch ordering technique. In this way, the selection of high resolution and low resolution pair patches $\{p_l^k, p_h^k\}_k$ is the first stage of the dictionary learning .Therefore, in the first step, the K-SVD training algorithm [14] is applied to low resolution patches $\{p_l^k\}_k$, that are selected by using the method which was described in pervious section, as a result, dictionary $\boldsymbol{D}_l$ is obtained:

$$\mathbf{D}_l, \{\alpha^k\} = \arg\min_{D_l, \{\alpha^k\}} \sum_k \left\| p_l^k - \mathbf{D}_l \alpha^k \right\|_2^2, \quad \text{X} \qquad (3)$$

$$s.t: \quad \left\| \alpha^k \right\|_1 \le s.$$

Since the dictionary learning problem is solved for both α and $\boldsymbol{D}_l$ and considering the basic assumption of the super resolution problem, both the HR and LR corresponding patch must have the same sparse representation vector. As a result, for HR patches $\{p_h^k\}_k$, we must have: $\{p_h^k\}_k \approx \boldsymbol{D}_h\{\alpha^k\}_k$.

Therefore, for high resolution dictionary $\boldsymbol{D}_h$we must have:

$$\mathbf{D}_h = \arg\min_{\mathbf{D}_h} \sum_k \left\| p_h^k - \mathbf{D}_h \alpha_i \right\|_2^2 = \arg\min_{\mathbf{D}_h} \sum_k \left\| \mathbf{P}_h - \mathbf{D}_h \mathbf{A} \right\|_2^2, \qquad (4)$$

Where, the matrix $\boldsymbol{P}_h$is constructed using the selected high-resolution training patches $\{p_h^k\}_k$ as its columns, and similarly $\boldsymbol{A}$ contains sparse representation vector for their paired low resolution patches over $\boldsymbol{D}_l$: $\{\alpha^k\}_k$ as its columns. The solution of the problem is given by the following Pseudo-Inverse expression [13] (given that Q has full row rank):

$$\mathbf{D}_h = \mathbf{P}_h \mathbf{A}^\dagger = \mathbf{P}_h \mathbf{A}^T \left(\mathbf{A}\mathbf{A}^T \right)^{-1}. \qquad (5)$$

3.2.1.HR image reconstruction

Given an LR image $\boldsymbol{Y} \in R^{N_1 \times N_2}$, we will establish an SR method based on patch ordering dictionary learning for reconstructing the HR image, $\boldsymbol{X} \in R^{fN_1 \times fN_2}$ where, $f$is the magnification scale. First, we divide LR image into patches $y \in R^{\sqrt{n} \times \sqrt{n}}$ by raster scanning. Considering that the sparse representation vectors for high and low resolution patch pairs must be the same regarding their corresponding dictionaries, it is suggested for any HR, LR image patches $x \in R^{\sqrt{n}f \times \sqrt{n}f}$ and $y \in R^{\sqrt{n} \times \sqrt{n}}$ the sparse representation model:

$$x \approx \mathbf{D}_h \alpha, \qquad y \approx \mathbf{D}_l \alpha; \tag{6}$$

Where, α is the coefficient vector of sparse representation which most entries are zero or close to zero. In order to restore x from y, y will be restored using the MMSE criteria in sparse condition.

$$\hat{\alpha} = \arg\min_{\alpha} \left\{ \left\| \mathbf{y} - \mathbf{D}_l \alpha \right\|_2^2 + \lambda \left\| \alpha \right\|_1 \right\}. \tag{7}$$

Greedy algorithms such as matching pursuit (MP) and orthogonal matching pursuit (OMP) [31] are used in order to find out the sparse representation vectors for each low resolution image patches. By applying the optimal solution for α to (4), the corresponding HR image patch x, is obtained simply by $\boldsymbol{D}_h \alpha$. After calculating all the HR image patches, a complete HR image $\mathbf{x}$ can be constructed by merging all these HR image patches using Yang merge global constraint [12].

3. EXPERIMENTAL RESULTS AND DISCUSSION

3.1. Test Bench

In order to compare the proposed SR algorithm with other algorithms, we compared our method with several classic and state of the art methods including bi-cubic interpolation, SCSR[12], SISU [13], ANR [33], GR[33], AMSRR [20] and SDS [21]. All the toolboxes of compared method are downloaded from their author's webpages. In order to have fair comparison, care has been taken to ensure that the parameters which were used in the methods are similar. Dataset selection is the first step of learning based on SR algorithm. In our experiment, the training images which were used by Yang et al. [12], (available at http://www.ifp.illinois.edu/~jyang29/) are selected for extracting HR and LR training patches. Testing was also done on two commonly used benchmark datasets (Set5 and Set14). In the next step, for HR and LR patches extraction, patches size and their overlap are the main parameters. For SCSR [12], the size of LR patches size is 5×5 with 4-th pixel overlap, corresponding HR patches which were obtained by implementing 4 high pass filters to HR image and concatenating 4 corresponding patches with 4- pixel overlap. The patch selection method is the same for SISU [13], the only difference is the dimension reduction which was applied using PCA algorithm in order to concatenated HR patches. In addition, other competing methods such as ANR [33] and GR[33] in dictionary learning phase were followed by SISU details [13]. Our patch selection in the proposed POSR algorithm uses 3×3 HR and LR patches with a 2-pixel overlap.

All of the experiments were performed using MATLAB R2014a on an Intel (R) Core (TM) i5-M 460 @2.53 GHz machine with 4 GB of RAM.

For assessment, we used the root mean square error (RMSE), peak signal-to- noise ratio (PSNR), structural similarity index (SSIM) and elapsed time as performance measures of the methods.

3.2. Results

We compared the performance of our proposed method with other state-of-the-art methods quantitatively and qualitatively by employing the processes, which were described in the previous sections. In our experiments, we magnified test images using bi-cubic interpolation, SCSR [12], SISU [13], ANR [33], GR [33] AMSRR [24], SDS [25] and our proposed POSR approach with a magnification factor of m = 3 and m = 4. As the human visual system is more sensitive to the change in luminance, the SR methods were only applied to the luminance channel of color images, and bi-cubic interpolation was used for the other channels.

For the magnification factor m=3, the comparison of the results of the values of PSNR, RMSE, SSIM and elapsed time by different methods are listed in Tables 2-5, also Tables 6- 9 shows results for m=4. These tables reveal that the proposed POSR method can possess better performance compared with some state-of-the-art methods.

For Visual comparison, Figs. 4-5 show image super resolution for butterfly and face images with magnification factor m=3, and Figs. 6-7 show more results for m=4, specific zoomed scenes were selected in order to clarify the comparison. We observed that bi-cubic and GR [33] methods tended to generate artifacts. Although, ANR [33], AMSRR [24] and SDS [25] methods improved visual details and edges. Compared to them, our proposed POSR method preserved sharp edges with more details in the images. Although the objective quality of a few HR images obtained by the proposed method has slightly advantage over the other methods, the average quantitative evaluations of proposed method are competitive to those of the others.

Moreover, according to Tables 5 and 9, the elapsed time of our algorithm is comparable with ANR [33] and GR [27], while its performance is much faster than other compared algorithms. Although, in terms of elapsed time our proposed algorithm is not the fastest method, it achieves satisfactory results. According to Table 5 in term of elapsed time, proposed method is faster than SCSR [12], SISU [13], and AMSRR [24], while is comparable with GR [33].

Comparing computational cost for the referring method, it can be observed that, in SCSR [12] method, HR training patches were obtained by implementing 4 high pass filters to HR images in order to extract high frequency features. Accordingly, after vectorization, they obtained LR patches with dimension 25×1, and HR patches with dimension 100×1, resulting in using these pair patches for dictionary training, which led to LR dictionary with dimension 25×1024 and HR dictionary with size100×1024. In SISU [13] method, which was proposed by Zeyde et al. by implementing a dimension reduction algorithm, HR patch dimension decreases from 100×1 to 30×1, also ANR [33], GR [33], AMSRR [24] and SDS [25] methods were followed by Zeyde et al.s̀ method. However, in our proposed POSR method, selected training patches were obtained from extracted patches that have been ordered by the proposed simple algorithm. Therefore, the structure of the proposed POSR method was much simpler in the learning stage. Moreover, since patch extraction method should be the same at the learning and reconstruction phase, the mentioned difference also can be observed in HR image reconstruction stage.

Therefore, POSR method had also simpler structure in reconstruction phase. Total evaluation for quantitative criteria (PSNR, RMSE, SSIM), human observation as a qualitative measure and also computational complexity comparison have verified the improvement of the proposed POSR algorithm.

4. CONCLUSION

In this paper, we presented a novel SISR algorithm based on dictionary learning and patch ordering. In the proposed method, all overlapping patches were extracted from each learning image and informative patches were selected using the proposed patch selection algorithm. This led to assigning more participation to images with more complex texture in dictionary learning stage. We presented results in order to demonstrate the effectiveness of the proposed method by comparing the number of selected patches with their TV measure. Although, in terms of elapsed time, our proposed algorithm is not the fastest method; it could achieve satisfactory results. Comparing the performance of the proposed POSR method quantitatively and qualitatively revealed that it was very competitive with the performance of state-of-the-art methods. The proposed patch selection and dictionary learning method can be also employed in order to sparse representation based on denoising and inpaiting.

Table 2. PSNR (dB) of the reconstructed HR images, where magnification factor m=3.

Benchmark	Set14							Set5			Average
Image	Lena	Barbara	Zebra	Baboon	Peppers	Sails	Coastguard	Parrot	Butterfly	Face	
Bicubic	29.80	26.91	21.56	25.21	29.83	25.72	26.79	30.69	24.58	33.88	27.49
SRSC[12]	30.88	27.40	23.13	25.50	31.48	26.38	26.80	30.94	25.48	34.31	28.23
SISU[13]	31.04	**27.86**	23.16	25.58	**31.91**	26.44	**27.30**	31.20	25.60	34.85	28.49
GR[33]	30.56	27.54	23.14	25.59	31.03	26.33	27.15	31.00	25.61	34.72	28.26
ANR[33]	31.11	27.83	23.28	**25.62**	31.80	**26.52**	27.23	31.20	25.77	34.94	28.53
AMSRR [24]	31.47	27.85	**23.27**	25.82	**24.12**	**26.56**	27.11	30.91	35.39	34.65	28.71
SDS[25]	31.60	27.80	23.21	25.72	23.98	26.51	27.09	30.88	34.78	34.66	28.62
proposed	**31.13**	27.76	**23.23**	25.51	31.69	26.26	**27.29**	**32.31**	**26.06**	**35.49**	**28.67**

Table 3. RMSE of the reconstructed HR images, where magnification factor m=3.

Benchmark	Set14							Set5			Average
Image	Lena	Barbara	Zebra	Baboon	Peppers	Sails	Coastguard	Parrot	Butterfly	Face	
Bicubic	8.24	11.49	19.98	13.98	8.22	13.19	11.66	7.44	15.04	5.15	11.43
SRSC[12]	7.28	10.86	17.77	13.53	6.79	12.23	11.66	7.23	13.55	4.90	10.58
SISU[13]	7.15	**10.31**	17.71	13.40	**6.45**	12.14	**11.00**	7.01	13.37	4.60	10.31
GR[33]	7.55	10.69	17.75	13.38	7.16	12.29	11.19	7.17	13.35	4.67	10.52
ANR[33]	7.09	10.34	**17.46**	**13.34**	6.55	**12.02**	11.08	7.87	13.11	4.56	10.34
AMSRR [24]	6.95	10.59	17.51	13.00	15.86	12.20	**11.07**	7.27	4.32	4.70	10.34
SDS[25]	6.71	10.52	17.58	13.11	16.20	12.22	11.16	7.30	4.50	4.71	10.40
proposed POSR	**7.07**	10.42	17.57	13.51	6.63	12.40	**11.01**	**6.17**	**12.69**	**4.28**	**10.17**

Table 4. SSIM of the reconstructed HR images, where magnification factor m=3.

Benchmark	Set14							Set5			Average
Image	Lena	Barbara	Zebra	Baboon	Peppers	Sails	Coastguard	Parrot	Butterfly	Face	
Bicubic	0.8422	0.7737	0.6914	0.6014	0.8968	0.6603	0.6064	0.8612	0.8412	0.8477	0.7622
SRSC[12]	0.8581	0.7976	0.7426	0.6414	0.9093	0.7060	0.6194	0.8607	0.8716	0.8490	0.7856
SISU[13]	0.8699	**0.8144**	0.7501	0.6465	**0.9248**	0.7101	0.6422	0.8751	0.8749	0.8678	0.7976
GR[33]	0.8592	0.7964	0.7549	**0.6563**	0.9084	0.7109	0.6428	0.8726	0.8761	0.8689	0.7947
ANR[33]	0.8720	0.8124	**0.7557**	0.6542	0.9232	**0.7160**	0.6424	0.8790	0.8793	0.8706	0.8005
AMSRR[24]	0.8701	0.8291	**0.7546**	**0.8808**	0.7659	**0.7165**	0.6427	0.8725	**0.9656**	**0.8611**	0.8159
SDS[25]	0.8698	0.8292	**0.7541**	**0.8794**	0.7564	0.7156	0.6423	0.8720	**0.9556**	**0.8668**	0.8141
proposed	**0.8741**	0.8112	0.7525	0.6540	0.9200	0.7096	**0.6533**	**0.8968**	**0.8827**	**0.8917**	**0.8046**

Table 5. Average elapsed time of the reconstructed HR images, magnification factor m=3 (Second).

Benchmark	Proposed POSR	SRSC[12]	SISU[13]	GR[33]	ANR[33]	AMSRR[24]	SDS[25]
Set 5	2.10	92.11	2.50	0.53	0.79	12.34	3.15
Set 14	1.99	89.29	2.55	0.48	0.71	12.93	3.06

Fig. 4. Visual comparison: (Top-left) Original HR image, (top-middle) Bicubic, (top-right) SCSR[12], (middle-left) SISU[13], (middle-middle) GR[33], (middle-right) ANR[33], (down-left) AMSRR[24], (down-middle) SDS [25], (down-right) proposed POSR, for magnification factor m=3.

Fig. 5. Visual comparison: (Top-left) Original HR image, (top-middle) Bicubic, (top-right) SCSR[12], (middle-left) SISU[13], (middle-middle) GR[27], (middle-right) ANR[27], (down-left) AMSRR[24], (down-middle)SDS [25], (down-right) proposed POS, for magnification factor m=3.

Table 9. Average elapsed time of the reconstructed HR images, magnification factor m=4 (Seconds).

Benchmark	Proposed POSR	SRSC[12]	SISU[13]	GR[33]	ANR[33]	AMSRR[24]	SDS[25]
Set 5	1.23	90.84	6.38	0.36	0.54	11.8	2.73
Set 14	1.19	70.47	1.82	0.55	0.62	10.53	1.86

Table 6. PSNR (dB) of the reconstructed HR images, where magnification factor m=4.

Benchmark	Set14							Set5			Average
Image	Lena	Barbara	Zebra	Baboon	Peppers	Sails	Coastguard	Parrot	Butterfly	Face	
Bicubic	27.88	25.62	20.03	24.39	27.59	24.21	25.84	29.74	24.39	32.24	26.02
SRSC[12]	27.71	25.56	20.14	24.34	27.80	24.23	25.73	29.32	24.34	31.61	25.94
SISU[13]	28.88	**26.60**	**20.54**	24.69	**29.44**	24.80	**26.22**	30.29	24.69	33.00	26.77
GR[33]	28.47	26.14	20.47	24.69	28.80	24.71	26.13	30.10	24.69	32.84	26.57
ANR[33]	28.90	26.38	20.53	**24.71**	29.33	**24.81**	26.18	30.26	**24.71**	33.05	26.75
AMSRR[24]	28.87	26.32	20.49	24.66	29.18	24.74	26.21	30.26	24.66	32.95	26.70
SDS[25]	28.76	26.27	20.48	24.63	29.10	24.67	26.11	30.17	24.63	32.85	26.63
proposed POSR	**29.16**	26.18	20.36	24.57	29.09	24.77	26.13	**31.29**	24.57	**33.37**	**26.85**

Table 7. RMSE of the reconstructed HR images, where magnification factor m=4.

Benchmark	Set14							Set5			Average
Image	Lena	Barbara	Zebra	Baboon	Peppers	Sails	Coastguard	Parrot	Butterfly	Face	
Bicubic	10.29	13.34	25.38	15.37	10.63	15.69	13.00	8.30	18.66	6.22	13.68
SRSC[12]	10.49	13.44	25.08	15.46	10.38	15.66	13.17	8.71	18.11	6.69	13.71
SISU[13]	9.16	**12.19**	**23.94**	14.85	**8.59**	14.66	**12.45**	7.79	17.37	5.70	12.67
GR[33]	9.61	12.56	24.14	14.85	9.25	**14.81**	12.57	7.96	17.27	5.81	12.88
ANR[33]	9.14	12.22	23.96	**14.81**	8.70	14.64	12.50	7.82	17.25	5.67	12.67
AMSRR[24]	9.17	12.30	24.09	14.91	8.85	14.77	12.46	7.82	17.33	5.73	12.74
SDS[25]	9.29	12.37	24.10	14.95	8.94	14.88	12.61	7.89	17.40	5.80	12.82
proposed POSR	**8.87**	12.50	24.54	15.08	8.95	14.71	12.60	**6.94**	**16.69**	**4.46**	**12.53**

Table 8. SSIM of the reconstructed HR images, where magnification factor m=4.

Benchmark	Set14							Set5			Average
Image	Lena	Barbara	Zebra	Baboon	Peppers	Sails	Coastguard	Parrot	Butterfly	Face	
Bicubic	0.7707	0.7025	0.5491	0.5112	0.8323	0.5494	0.5287	0.8278	0.7540	0.8002	0.6826
SRSC[12]	0.7624	0.7061	0.5472	0.5057	0.8446	0.5525	0.5166	0.8092	0.8716	0.7805	0.6896
SISU[13]	0.8014	**0.7435**	0.6016	0.5489	**0.8764**	0.5996	0.5557	0.8424	0.7876	0.8187	0.7176
GR[33]	0.7860	0.7248	0.6040	**0.5562**	0.8555	**0.6008**	0.5585	0.8396	0.7924	0.8177	0.7136
ANR[33]	0.8021	0.7412	0.6049	0.5546	0.8729	0.6031	0.5568	0.8432	0.7913	0.8208	0.7191
AMSRR[24]	0.8005	0.7390	0.5954	0.5474	0.8706	0.5951	0.5542	0.8415	0.7876	0.8172	0.7148
SDS[25]	0.7961	0.7330	0.5966	0.5455	0.8669	0.5907	0.5504	0.8397	0.7857	0.8153	0.7120
proposed	**0.8113**	0.7339	**0.6085**	0.5537	0.8629	0.6006	**0.5592**	**0.8660**	**0.7981**	**0.8421**	**0.7236**

Fig. 6. Visual comparison: (Top-left) Original HR image, (top-middle) Bicubic, (top-right) SCSR[12], (middle-left) SISU[13], (middle-middle) GR[33], (middle-right) ANR[33], (down-left) AMSRR[24], (down-middle) SDS [25], (down-right) proposed POSR, for magnification factor m=3.

Fig. 7. Visual comparison: (Top-left) Original HR image, (top-middle) Bicubic, (top-right) SCSR[12], (middle-left) SISU[13], (middle-middle) GR[33], (middle-right) ANR[33], (down-left) AMSRR[24], (down-middle) SDS [25], (down-righ) proposed POSR, magnification factor m=4.

REFERENCES

[1] Dai S, Han M.,Xu W, et al. **"Soft edge smoothness prior for alpha channel super resolution"**. *In: Proceeding of the 2007 IEEE Conf. Computer Vision and Pattern Recognition*, pp.1-8, 2007.

[2] Sun J, Xu Z, Shum H., **"Image super-resolution using gradient profile prior".** *In: Proceeding of the 2008 IEEE Conf. Computer Vision and Pattern Recognition*, pp.1-8, 2008.

[3] Chen H, Jiang B, Chen B., **"Image super-resolution based on patches structure".** *In: Proceeding of the 2011 IEEE International Congress Image and Signal Processing*, pp. 1076-1080, 2011.

[4] Farsiu S, Robinson M. D, Elad M, et al. **"Fast and robust multi-frame super resolution".** *IEEE Trans. Image Process.* , Vol. 13(10), pp. 1327-1344, 2004.

[5] Hardie R.C, Barnard K.J, Armstrong E.E, **"Joint MAP registration and high-resolution image estimation using a sequence of under sampled images".** *IEEE Trans. Image Process*. Vol. 6(12), pp. 1621-1633.6, 1997.

[6] Jiang J, Hu R, Han, Z, et al. **"Efficient single image super-resolution via graph-constrained least squares regression".** *Multimedia Tools and Applications*, Vol. 72(3), pp. 2573-2596, 2014.

[7] Suresh K.V, Rajagopalan A. **"A discontinuity adaptive method for super-resolution of license plates".** *Computer Vision, Graphics and Image Process*. pp. 25-34. 2006.

[8] Freeman W.T, Jones T.R, Pasztor E.C., **"Example-based super-resolution"**, *IEEE Computer graphics and Applications*, Vol. 22(2), pp. 56-65, 2002.

[9] Gao X, Zhang, K, Tao D, Li X, **"Image Super-Resolution with Sparse Neighbor Embedding"**, *IEEE Trans. of Image Process*. Vol. 21(7), pp. 3194-3205, 2012.

[10] Yang J, Wang Z, Lin Z, Cohen S, Huang T., **"Coupled Dictionary Training for Image Super-Resolution".** *IEEE Trans. Image Process*. Vol. 21(8), pp. 3467-3478, 2012.

[11] Yang J, Wright J, Huang T, Ma Y., **"Image super-Resolution as Sparse Representation of Raw Image Patches",** *In: Proceeding of the IEEE Conference on Computer Vision and Pattern Recognition*, pp. 1-8, 2008.

[12] Yang J, Wright J, Huang T, Ma Y., **"Image Super-Resolution Via Sparse Representation",** *IEEE Trans. on image Process.*Vol. 19(11), pp. 2861-2873, 2010.

[13] Zeyde R, Elad M, Protter M, **"On Single Image Scale-Up Using Sparse-Represe*ntations"*,** *Lecture Notes in Computer Science*, Vol. 69(20), pp. 711-730, 2012.

[14] Aharon M, Elad M, Bruckstein A., **"A K-SVD: An Algorithm for Designing Overcomplete Dictionaries for Sparse Representation"**, *IEEE Trans. on Signal Process*, Vol. 54(11), pp. 4311-4322

[15] Cao F, et al. **"Image Super-Resolution via Adaptive l_p (o<p<1) Regularization and Sparse Representation",** *IEEE Trans. on Neural Networks and Learning Systems*, Vol. 27(7), pp. 1550-1561, 2016.

[16] Gong W, HU L, Li J, Li W., **"Combining Sparse Representation and Local Rank Constraint for Single Image Super Resolution",** *Information Sciences*, 325. pp. 1-19, 2015.

[17] Han N, Song Z, Li Y., **"Cluster-based Image Super-Resolution via Jointly Low-Rank and Sparse Representation",** *Journal of Visual Communication and Image Representation*, Vol. 38, pp. 175-185, 2016.

[18] Wang S, Zhang L, Liang Y, Pan Q., **"Semi-coupled Dictionary learning with applications to Image Super-Resolution and Photo-Sketch Synthesis",** *In: proceeding of the IEEE Conf. Computer Vision and Pattern Recognition*, pp. 2216-2223, 2012.

[19] Liu D, Wang Z, Wen B, Yang J, Han W., **"Huang, T. Robust Single Image Super-Resolution Via Deep Networks with Sparse Prior"**, *IEEE Trans. on Image Process.* Vol. 25(7), pp. 3194-3207, 2016.

[20] Yeganli F, Nazzal M, Unal M, Ozkaramanli H., **"Image Super-Resolution Via Sparse Representation Over Coupled Dictionary Learning Based On Patch Sharpness",** *In: Proceeding of the IEEE European Modelling Symposium*, pp.203-208, 2012.

[21] Chao G, Bo J, Ai-xin Z., **"MCA-based Image Super Resolution",** *Communications Technology*, Vol. 3, pp. 20-27, 2013.

[22] Jiang J, Yang J, Pan Z., **"Super-resolution Reconstruction based on Structure Tensor's Eigenvalue and Classification Dictionary",** In: *Proceeding of the Int. Conf. on in Audio, Language and Image Processing*, pp. 452-456, 2016.

[23] Liu M, Chen X, Wang X., **"Latent Fingerprint Enhancement via Multi-Scale Patch based Sparse Representation",** *IEEE Trans. on Information Forensics and Security*, Vol. 10(1), pp. 6-15.24, 2015.

[24] Zhang H, Liu W, Liu J, Liu C, Shi C., **"Sparse Representation and Adaptive Mixed Samples regression for Single Image Super-Resolution",** *Signal Process: Image Communication*. 67: pp. 79-89, 2018.

[25] Lu W, Sun H, Wang R, He L, Jou M, Syu S, Li J. **"Single Image Super Resolution Based On Sparse Domain Selection",** *Neurocomputing*. 269: pp. 180-187, 2017.

[26] Naderahmadian Y, Beheshti S, Tinati M. A., **"Correlation Based Online Dictionary Learning Algorithm"**, *IEEE Trans. on Signal Process*. Vol. 64(3), pp. 592-602, 2016.

[27] Zhu X, Tao J, Li B, Chen X, Li Q., **"A Novel Image Super-Resolution Reconstruction Method Based On Sparse Representation Using Classified Dictionaries",** *In: Proceeding of the IEEE International Conference on Information and Automation*, pp.776-780, 2015.

[28] Yang W, Yuan T, Wang W, Zhao F, Liao Q., **"Single-Image Super-Resolution by Subdictionary Coding and Kernel Regression",** I*EEE Trans. on Systems, Man and Cybernetics: Systems*, Vol. 47(9), pp. 2478-2488, 2017.

[29] Juefei-Xu F, M Savvides, **"Single Face Image Super-Resolution via Solo Dictionary Learning",** *In: Proceeding of the IEEE International Conference on Image Processing (ICIP)*, pp. 2239-2243, 2015.

[30] Ram I, Elad M, Cohen I., **"Image Processing Using Smooth Ordering of its Patches'"**, *IEEE Trans. on Image Process*. Vol. 22(7), pp. 2764-2774, 2013.

[31] Cormen T.H. **"Introduction to Algorithms (2nd ed.)"**, *MIT press*, 2009.

[32] Pati Y.C, Rezaiifar R, Krishnaprasad P.S., **"Orthogonal Matching Pursuit: Recursive Function Approximation with Applications to Wavelet Decomposition",** *In Proceedings of 27th Asilomar Conference on Signals, Systems and Computers*, pp. 40-44.27, 1993.

[33] Timofte R, De Smet V, Van Gool L., **"Anchored Neighborhood Regression for Fast Example-Based Super-Resolution",** *In: Proceeding of the IEEE International Conference on Computer Vision, Sydne*y, pp. 1920-1927, 2013.